

Research Article

Reliability Monitoring of Fault Tolerant Control Systems with Demonstration on an Aircraft Model

Hongbin Li,¹ Qing Zhao,¹ and Zhenyu Yang²

¹ Department of Electrical and Computer Engineering, University of Alberta, Edmonton, AB, Canada T6G 2V4

² Department of Computer Science and Engineering, Aalborg University Esbjerg, Niels Bohrs Vej 8, 6700 Esbjerg, Denmark

Correspondence should be addressed to Qing Zhao, qingzhao@ece.ualberta.ca

Received 4 April 2007; Revised 6 September 2007; Accepted 13 November 2007

Recommended by Kemin Zhou

This paper proposes a reliability monitoring scheme for active fault tolerant control systems using a stochastic modeling method. The reliability index is defined based on system dynamical responses and a safety region; the plant and controller are assumed to have a multiple regime model structure, and a semi-Markov model is built for reliability evaluation based on the safety behavior of each regime model estimated by using Monte Carlo simulation. Moreover, the history data of fault detection and isolation decisions is used to update its transition characteristics and reliability model. This method provides an up-to-date reliability index as demonstrated on an aircraft model.

Copyright © 2008 Hongbin Li et al. This is an open access article distributed under the Creative Commons Attribution License, which permits unrestricted use, distribution, and reproduction in any medium, provided the original work is properly cited.

1. INTRODUCTION

In order to meet high reliability requirement of safety-critical processes, major progress has been made in fault tolerant control systems (FTCSs). FTCSs usually employ fault detection and isolation (FDI) schemes and reconfigurable controllers to accommodate fault effects, also known as active FTCSs. Most work on reconfigurable controller design is performed under the assumption of perfect FDI detections. However, imperfect FDI results are inevitable owing to disturbances or modeling uncertainties and may corrupt designated reliability requirement. Therefore, it is necessary to validate the design of FTCSs from a reliability perspective.

The reliability of FTCSs has been investigated using various methods. The key problem is to set up appropriate reliability models with control objectives and safety requirements incorporated. As fault occurrences and system failures are rare events, dynamic models are usually not suitable for reliability analysis. For example, Wu used serial-parallel block diagrams and Markov models for evaluation purpose, and defined a coverage concept to relate reliability and control actions [1]. Walker proposed Markov and semi-Markov models to describe the transitions of fault and FDI modes, but control actions are not considered [2]. In previous work,

we considered static model-based control objectives and built a semi-Markov model from imperfect FDI and hard-deadline concepts [3, 4]. However, in many practical systems, the safety and reliability of operation are often assessed based on dynamic system responses. For instance, reliability in structural control is defined as the probability of system outputs outcrossing safety boundaries and evaluated by using Gaussian approximation [5]. Also, an online available reliability monitoring scheme using updated information may aid maintenance scheduling, provide prealarms, and avoid emergent overhauls. How to evaluate reliability when it is defined based on system trajectory and how to implement an online-monitoring scheme are the main motivations of this paper.

The objectives of this paper are threefold. First of all, a steady-state test (SST) is proposed to reduce false alarms of FDI decisions. The stochastic modeling of such an FDI scheme is studied based on which the transition characteristics of FDI modes can be described. The second objective is to develop a reliability evaluation scheme for FTCSs based on system dynamic responses and safety boundary. At last, online monitoring features are considered, such as estimation of FDI transition parameters based on history data and timely update of reliability index to reflect up-to-date system behavior.

The remainder of this paper is organized as follows: the assumptions and system structure are given in Section 2; FDI scheme, modeling, and parameter estimation are discussed in Section 3; the determination of outcrossing failure rates and hard-deadlines are discussed in Section 4; the reliability model construction is discussed in Section 5 followed by a demonstration example of an F-14 aircraft model in Section 6.

2. ASSUMPTIONS AND SYSTEM STRUCTURE

Assumption 1. The considered plant is assumed to have finite fault modes, and dynamics under each fault mode can be effectively represented by a linear system model.

Fault modes are represented by a set S with N integers; $\{\mathcal{M}_i : i \in S\}$ represents the set of dynamical plant models under various fault modes; $\{\mathcal{K}_j : j \in S\}$ denotes a set of reconfigurable controllers in a switching structure. \mathcal{K}_j is designed for fault mode j based on \mathcal{M}_j , $j \in S$. However, true fault modes are usually not directly known, so an FDI scheme is used to generate estimates of fault modes, which may deviate from true fault modes with error probabilities.

Assumption 2. FDI scheme is assumed to generate a fault estimate based on a batch of measurements and calculations for every fixed period T_c .

This assumption states a cyclic feature of FDI, such as statistical tests and interactive multiple model (IMM) Kalman filters [6]. FDI modes are represented by a discrete-time stochastic process $\eta_n \in S$, where $n \in \mathbb{N}$, the set of nonnegative integers. The time duration between consecutive discrete indices is equal to FDI detection period T_c . \mathcal{K}_j is put in use when $\eta_n = j$, $j \in S$. Corresponding to η_n , a discrete-time stochastic process ζ_n denotes true fault mode. In reliability engineering, constant failure rates are usually assumed for the main part of component life cycle. In such a case, ζ_n can be described as a Markov chain [7], and its transition probabilities are denoted as $G_{ij} = \Pr\{\zeta_{n+1} = j \mid \zeta_n = i\}$, $i, j \in S$.

Remark 1. The semi-Markov process can be used as a general FDI model. It can describe any type of sojourn time distribution; in contrast, the Markov process model accepts exponential sojourn time distributions only. More discussions can be found in [4].

Assumption 3. System performance is assumed to be represented by a vector signal $z(t)$. Safety region, denoted as Ω , is assumed to be a fixed region in the space of $z(t)$ bounded by its safety threshold. Failure is assumed to occur when $z(t)$ exceeds a safety region for the first time.

This assumption intends to define an appropriate reliability index based on system dynamical response. It is common in control systems to use a signal $z(t)$ to represent performance, and $z(t)$ is usually to be kept at small values against influences from exogenous disturbances, modeling uncertainties, and dynamical characteristic changes caused

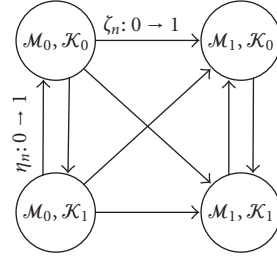


FIGURE 1: Transitions among regime models.

by faults. Safety region Ω is assumed to be fixed and known a priori. The scenario that $z(t)$ exceeds Ω represents lost of control and system failures. More discussions on this assumption can be found in [8].

Definition 1. For a time interval from 0 to t , the reliability function $R(t)$ is defined as the following probability:

$$R(t) = \Pr\{\forall 0 \leq \tau \leq t, z(\tau) \in \Omega\}. \quad (1)$$

Mean time to failure (MTTF) is defined as the expected time of satisfactory operation:

$$\text{MTTF} = \int_0^\infty R(t) dt. \quad (2)$$

Remark 2. Different from repairs relying on human intervention when system operation is stopped, control actions are executed automatically and can be deemed as an internal actions of FTCs. Therefore, MTTF represents the mean operational time without human intervention before failure.

Compared with ζ_n and η_n , $z(t)$ is typically a fast changing function determined by both continuous and discrete dynamics. As shown in Figure 1, ζ_n and η_n are two regime modes and determine the transitions among regime models. When $\zeta_n = i$ and $\eta_n = j$ are fixed, $z(t)$ evolves according to plant model \mathcal{M}_i and controller \mathcal{K}_j . As a result of this hybrid dynamics, directly evaluating $R(t)$ and MTTF is a difficult problem. Therefore, a discrete-time semi-Markov chain X_n is constructed for reliability evaluation purpose. The main idea is that the hybrid system is decomposed into various regime models; each regime model is then evaluated for related safety characteristics, and X_n is constructed to integrate these characteristics with transition parameters of regime modes and to solve its transition probabilities for reliability evaluation. The structure and main components of reliability monitoring scheme are illustrated in Figure 2.

Semi-Markov reliability model X_n is the kernel component for calculating MTTF. It is constructed based on the following parameters: (1) the transition rates of ζ_n , called plant failure rates, (2) the estimates of ζ_n from FDI and confirmation test, called confirmed fault modes, (3) the parameters of η_n estimated from history data, called FDI transition characteristics, (4) the probability of $z(t)$ crossing safety boundary during an FDI cycle T_c when $\zeta_n = \eta_n$, called failure outcrossing rates, (5) the average number of periods before crossing safety boundary when $\zeta_n \neq \eta_n$, called hard deadlines. Among

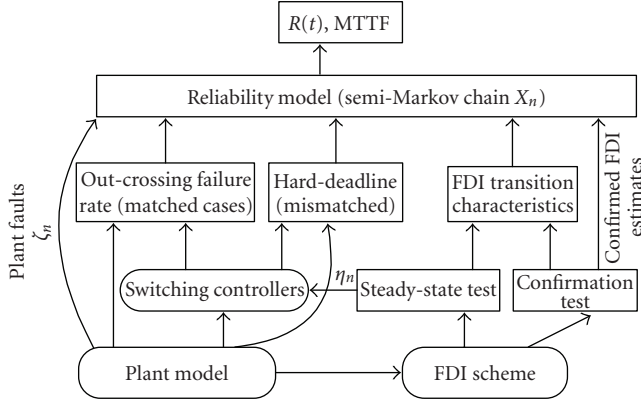


FIGURE 2: System structure.

these parameters, the second and third ones can be updated online.

3. FDI SCHEME AND ITS CHARACTERIZATION

3.1. Steady-state tests

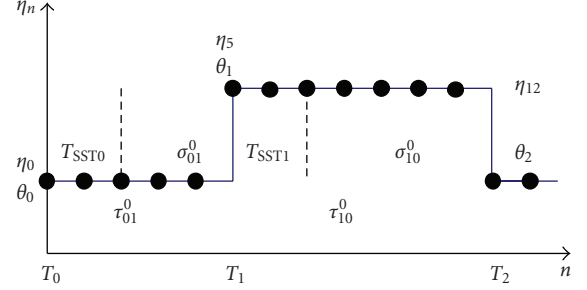
It is well known that false alarm and missing detection rates are two conflicting quality criteria of FDI. One is usually improved at the cost of degrading the other. What is worse, the general rules of adjusting FDI to improve these two criteria simultaneously are often not known. For example, in a scheme based on IMM Kalman filters, it is not clear how to determine Markov interaction parameters. Considering that most false alarms last for short time only, an SST strategy is adopted for postprocessing FDI decisions.

SST requires that, when FDI decision changes, new decision is accepted only when it stays the same for a minimum number of detection cycles. Let T_{SSTj} denote the required number of consistent cycles for FDI mode j , $j \in S$. The effectiveness of this SST strategy relies on the distribution of false alarm durations. For example, if a nonnegative discrete random variable λ_0 denotes the false alarm duration when system fault mode $\zeta_n = 0$, T_{SST0} can be taken as $(1 - \alpha)$ -quantile of λ_0 , $0 < \alpha < 1$, meaning

$$\Pr\{\lambda_0 > T_{SST0}\} \leq \alpha, \quad (3)$$

which implies that false alarm probability can be reduced by ratio α when accepting FDI decisions after T_{SST0} . The weakness of this method is additional detection time delay of T_{SSTj} when fault occurs. However, this happens only under rare occurrences of faults. Compared with the improvement on relatively more frequently transitions of FDI modes, this weakness is acceptable.

Detection decisions from SST are represented by η_n and used for controller reconfigurations. In Figure 2, the confirmation test is an SST with large test period to further reduce false alarm probability to a negligible level. It generates confirmed fault modes, which are used with FDI trajectories for updating transition parameters of η_n and reliability index.

FIGURE 3: A sample path of η_n .

3.2. Stochastic models

A sample path of η_n is given in Figure 3. Let $\theta_m \in S$ and $T_m \in \mathbb{N}$ denote the FDI mode and cycle index, respectively, after the m th transition of η_n , $m \in \mathbb{N}$. For example, in Figure 3, $\theta_1 = \eta_5$ and $T_2 = 5$. θ_m and T_m together determine FDI trajectory, and $\eta_n = \theta_{S_n}$, where $S_n = \sup\{m \in \mathbb{N} : T_m \leq n\}$ is the discrete-time counting process of the number of jumps in $[1, n]$. $(\theta, T) \triangleq \{\theta_m, T_m : m \in \mathbb{N}\}$ is called a discrete-time Markov renewal process if

$$\begin{aligned} \Pr\{\theta_{m+1} = j, T_{m+1} - T_m = l \mid \theta_0, \dots, \theta_m; T_0, \dots, T_m\} \\ = \Pr\{\theta_{m+1} = j, T_{m+1} - T_m = l \mid \theta_m\} \end{aligned} \quad (4)$$

holds for fixed $\zeta_{T_m} = \zeta_{T_{m+1}} = \dots = \zeta_{T_{m+1}} = k$, $k, j \in S$, $l, m \in \mathbb{N}$. $\eta_n = \theta_m$ is then called the associated discrete-time semi-Markov chain of (θ, T) . It can be shown that θ_m is a Markov chain, and its transition probability matrix is denoted by P^k .

Given $\zeta_{T_m} = \zeta_{T_{m+1}} = \dots = \zeta_{T_{m+1}} = k$, let $\tau_{ij}^k = T_{m+1} - T_m$ if $\theta_m = i$ and $\theta_{m+1} = j$, $i, j, k \in S$. τ_{ij}^k is the sojourn time of η_n between its transition to state i at T_m and the consecutive transition to j at T_{m+1} . If the transition destination state is not specified, let τ_i^k denote the sojourn time at state i .

As shown in Figure 3, τ_{ij}^k is the sum of two variables: a constant T_{SSTi} for SST period and a random sojourn time σ_{ij}^k . Let $h_{ij}^k(l)$ and $g_{ij}^k(l)$ denote the discrete distribution functions of τ_{ij}^k and σ_{ij}^k respectively, which have the following relations:

$$h_{ij}^k(l) = \Pr\{\tau_{ij}^k = l\} = \begin{cases} 0, & l \leq T_{SSTi}, \\ g_{ij}^k(l - T_{SSTi}), & l > T_{SSTi}. \end{cases} \quad (5)$$

This semi-Markov description provides a general model on FDI mode transitions, but it involves a large number of parameters. The transition characteristics of η_n are jointly determined by P^k and h_{ij}^k (or g_{ij}^k). If S contains N fault modes, there are N transition probability matrices P^k and N^3 distribution functions h_{ij}^k . If each h_{ij}^k follows geometric distribution, the description of η_n may degenerate to a hypothetical Markov model η'_n .

All Markov chains can be considered as a special type of semi-Markov chains. If η_n can be modeled as a Markov chain

with transition probability matrix denoted by H^k for $\zeta_n = k$, the following relations hold:

$$P_{ij}^k = \frac{H_{ij}^k}{1 - H_{ii}^k}, \quad (6)$$

$$h_{ij}^k(l) = (H_{ii}^k)^{l-1} H_{ij}^k, \quad (7)$$

$$h_i^k(l) = (H_{ii}^k)^{l-1} (1 - H_{ii}^k). \quad (8)$$

It is obvious that h_i^k is a geometric distribution. In fact, this is an essential property of Markov chain, as shown in the following lemma.

Lemma 1. *A discrete-time semi-Markov chain degenerates to a Markov chain if and only if the sojourn time at each state (when subsequent state is not specified) follows geometric distribution.*

The proof is given in the appendix. When T_{SST} is nonzero, the sojourn time of η_n does not follow geometric distribution owing to this deterministic constant, and Lemma 1 cannot be directly applied. However, as T_{SST} is known, a hypothetical process η'_n can be constructed by setting T_{SST} to zeros; if the sojourn time of η'_n is geometrically distributed, it can be described as a Markov chain; the original sojourn time of η_n can be recovered by adding T_{SST} to that of η'_n . This method may greatly reduce the number of parameters for characterizing FDI results.

3.3. Transition parameter estimation

FDI transition parameters can be estimated as an offline test on FDI when both fault mode and FDI detection results are known. This estimation can also be carried out online using FDI history data and confirmed fault modes.

When η_n is modeled as a semi-Markov chain, P^k and h_{ij}^k (or g_{ij}^k) are parameters to be estimated. P^k can be estimated from the transition history of η_n . For example, when ζ_n is kept as a constant k , if there are M_{ij} transitions from i to j among all M transitions leaving i , the ij th element of P^k can be estimated as $\hat{P}_{ij}^k = M_{ij}/M$.

The estimation of sojourn time distribution g_{ij}^k can be completed in two steps: the histogram of sojourn time is firstly examined to select a standard distribution such that nonparametric estimation is converted to a parametric one; \hat{g}_{ij}^k is then obtained by estimating unknown parameters in distribution functions.

If \hat{g}_{ij}^k follows geometric distribution for all $i, j, k \in S$, η_n can be described as a hypothetical Markov chain η'_n under the hypothesis that $T_{SSTi} = 0$. As a result, transition probability H_{ij}^k from i to j and sojourn time τ_i^k at i have the following relation:

$$\Pr\{\tau_i^k = n\} = (H_{ii}^k)^{n-1} (1 - H_{ii}^k). \quad (9)$$

Therefore, $E(\tau_i^k) = 1/(1 - H_{ii}^k)$, and H_{ii}^k can be estimated by

$$\hat{H}_{ii}^k = \begin{cases} 1 - \frac{1}{\sum_{l=1}^M \tau_i^k(l)/M}, & \sum_{l=1}^M \tau_i^k(l) \neq 0, \\ 1, & \text{otherwise,} \end{cases} \quad (10)$$

where $\tau_i^k(l)$ denote M sojourn time samples at state i , $l = 1, \dots, M$. H_{ij}^k can be estimated based on the transition frequency from state i to j :

$$\hat{H}_{ij}^k = \frac{(1 - \hat{H}_{ii}^k) w_{ij}^k}{M}, \quad (11)$$

where $1 - \hat{H}_{ii}^k$ is a normalization coefficient and w_{ij}^k represents the number of FDI transitions from i to j .

4. OUTCROSSING FAILURE RATES AND HARD-DEADLINES

Owing to FDI delays or incorrect decisions, controller \mathcal{K}_i may be used for its designated regime model \mathcal{M}_i (namely, matched cases) and other model \mathcal{M}_j , $i \neq j$ (namely, mismatched cases). Matched cases usually account for major operation time, while mismatched cases often appear as temporary operation.

Definition 2. The outcrossing failure rate in matched cases is defined as

$$v_{ii} \triangleq \Pr\{\exists \tau, nT_c < \tau \leq (n+1)T_c, \\ z(\tau) \notin \Omega \mid z(nT_c) \in \Omega, \zeta_n = \eta_n = i\}, \quad i \in S. \quad (12)$$

Monte Carlo simulation can be used for estimating v_{ii} : sample simulations are performed by using generated sample uncertain plant model and sample disturbance input; the simulation time when system fails is called a sample time-to-failure. With a large number of time-to-failure samples obtained, v_{ii} can be estimated as the ratio between T_c and sample mean of time-to-failure.

Mismatched cases are usually temporary operation caused by FDI false alarms or delays, and system may return to matched cases if $z(t)$ does not diverge to unsafe region. So, it is important to find out the average tolerable time before system failure. This time limit is called hard-deadline, denoted by T_{hdij} for $\zeta_n = i$ and $\eta_n = j$. It can also be estimated by sample mean of time-to-failure using Monte Carlo simulations.

5. RELIABILITY MODEL CONSTRUCTION

The states of semi-Markov chain X_n for reliability evaluation are classified into two groups: one unique failure state, denoted by s_F , and multiple functional states, defined as state combinations of $\zeta_n = i$ and $\eta_n = j$, denoted as s_{ij} , $i, j \in S$. For example, if two types of faults are considered in the plant, ζ_n includes states of fault-free, fault type 1, fault type 2, and both fault 1 and fault 2, represented by $S = \{0, 1, 2, 3\}$, and X_n contains 17 states.

The semi-Markov kernel of X_n is denoted as $Q(\cdot, \cdot, m)$, representing the one-time transition probability in m cycles. It is determined by the following parameters: (1) transition characteristics of fault and FDI modes, (2) outcrossing failure rate in state s_{ii} denoted by v_{ii} , (3) hard-deadline in state s_{ij} denoted by T_{hdij} , (4) FDI SST period denoted by T_{SSTj} for FDI mode j .

Let us begin with the case that FDI mode can be described as a hypothetical Markov chain η'_n with transition probability denoted by H_{ij}^k . The calculation of Q is classified into the following cases.

Case 1. The transitions from functional states to themselves are not defined and the corresponding elements are assigned as zeros:

$$Q(s_{ii}, s_{ii}, m) = 0, \quad Q(s_{ij}, s_{ij}, m) = 0, \quad i, j \in S. \quad (13)$$

Case 2. Failure state s_F is absorbing:

$$Q(s_F, s_F, m) = \begin{cases} 1, & m = 1, \\ 0, & m > 1. \end{cases} \quad (14)$$

Case 3. Initial states are matched states s_{ii} :

$$\begin{aligned} Q(s_{ii}, s_F, m) &= \begin{cases} (1 - v_{ii})^{m-1} G_{ii}^{m-1} v_{ii}, & m \leq T_{SSTi}, \\ p_{ii} [(1 - v_{ii}) G_{ii} H_{ii}^i]^{(m-T_{SSTi}-1)} v_{ii}, & m > T_{SSTi}, \end{cases} \\ Q(s_{ii}, s_{jj}, m) &= \begin{cases} (1 - v_{ii})^{m-1} G_{ii}^{m-1} (1 - v_{ii}) G_{ij}, & m \leq T_{SSTi}, \\ p_{ii} [(1 - v_{ii}) G_{ii} H_{ii}^i]^{(m-T_{SSTi}-1)} (1 - v_{ii}) G_{ij} H_{ij}^i, & m > T_{SSTi}, \end{cases} \\ Q(s_{ii}, s_{ij}, m) &= \begin{cases} 0, & m \leq T_{SSTi}, \\ p_{ii} [(1 - v_{ii}) G_{ii} H_{ii}^i]^{(m-T_{SSTi}-1)} (1 - v_{ii}) G_{ij} H_{ij}^i, & m > T_{SSTi}, \end{cases} \\ Q(s_{ii}, s_{kj}, m) &= \begin{cases} 0, & m \leq T_{SSTi}, \\ p_{ii} [(1 - v_{ii}) G_{ii} H_{ij}^k]^{(m-T_{SSTi}-1)} (1 - v_{ii}) G_{ik} H_{ij}^i, & m > T_{SSTi}, \end{cases} \end{aligned} \quad (15)$$

where $p_{ii} = \Pr\{X_1 = X_2 = \dots = X_{T_{SSTi}} = s_{ii} \mid X_0 = s_{ii}\} = (1 - v_{ii})^{T_{SSTi}} G_{ii}^{T_{SSTi}}$, $i \neq j, k \neq i, i, j, k \in S$.

The derivation of these equations are based on Markov transition probabilities and the decomposition of each event. For example,

$$\begin{aligned} Q(s_{ii}, s_F, m) &= \Pr\{X_1 = X_2 = \dots = X_{m-1} = s_{ii}, X_m = s_F \mid X_0 = s_{ii}\} \\ &= \Pr\{X_1 = X_2 = \dots = X_{m-1} = s_{ii} \mid X_0 = s_{ii}\} \\ &\quad \times \Pr\{X_1 = s_F \mid X_0 = s_{ii}\}. \end{aligned} \quad (16)$$

Considering the SST of FDI, if $m \leq T_{SSTi}$,

$$\begin{aligned} \Pr\{X_1 = X_2 = \dots = X_{m-1} = s_{ii} \mid X_0 = s_{ii}\} \\ = (1 - v_{ii})^{m-1} G_{ii}^{m-1}. \end{aligned} \quad (17)$$

If $m > T_{SSTi}$,

$$\begin{aligned} \Pr\{X_1 = X_2 = \dots = X_{m-1} = s_{ii} \mid X_0 = s_{ii}\} \\ = \Pr\{X_1 = X_2 = \dots = X_{T_{SSTi}} = s_{ii} \mid X_0 = s_{ii}\} \\ \quad \times [(1 - v_{ii}) G_{ii} H_{ii}^i]^{(m-T_{SSTi}-1)}. \end{aligned} \quad (18)$$

$Q(s_{ii}, s_F, m)$ can be obtained by combining these two probabilities with $\Pr\{X_1 = s_F \mid X_0 = s_{ii}\} = v_{ii}$.

Case 4. Mismatched states, s_{ij} , $i \neq j$. When $m \leq T_{SSTj}$, the transition probability of $X(t)$ to any other state is zero because of SST period. When $T_{SSTj} < m \leq T_{hdij}$, the probability of $X(t)$ transiting to any other state is zero except to s_{ii} . The above reasoning is based on the facts that FDI rarely jumps to other false modes when current mode is incorrect, and mean fault occurrence time is in a much higher order compared with a short false FDI detection period. Therefore, when $T_{SSTj} < m \leq T_{hdij}$,

$$\begin{aligned} Q(s_{ij}, s_F, m) &= 0, \\ Q(s_{ij}, s_{ii}, m) &= (H_{jj}^i)^{m-T_{SSTj}-1} H_{ji}^i, \quad j \neq l, j, l \in S. \end{aligned} \quad (19)$$

When $m > T_{hdij} + 1$, X_n jumps to s_F at the earliest time $m = T_{hdij} + 1$ only:

$$\begin{aligned} Q(s_{ij}, s_F, T_{SSTi} + 1) &= 1 - \sum_{k=T_{SSTi}+1}^{T_{hdij}} Q(s_{ij}, s_{ii}, m) \\ &= 1 - \frac{1 - (H_{jj}^i)^{T_{ij}-T_{SSTj}+1}}{1 - H_{jj}^i} H_{ji}^i. \end{aligned} \quad (20)$$

In the general cases, η_n is modeled as a semi-Markov chain, and the competition probabilities methods discussed in [4] can be utilized.

Definition 3. Given $\zeta_n = i$ and $\eta_n = j$, the combinational mode is denoted as (i, j) , $i, j \in S$. Suppose $(\zeta_{n+1}, \eta_{n+1}) = \dots = (\zeta_{n+m-1}, \eta_{n+m-1}) = (i, j)$ and the next combinational mode after the consequent transition of ζ_n or/and η_n at $n+m$ is $(\zeta_{n+m}, \eta_{n+m}) = (k, l)$, where $k \neq i$ or/and $l \neq j$, $k, j \in S$. The probability of this event is called the competition probability, denoted by $\rho_{(i,j) \rightarrow (k,l)}(m)$.

The calculation formulas of $\rho_{(i,j) \rightarrow (k,l)}(m)$ were derived in [4, Section 3] and are omitted here for brevity. As the states of X_n are mainly defined as the state combinations of ζ_n and η_n , the calculation of the semi-Markov kernel of X_n is simplified when $\rho_{(i,j) \rightarrow (k,l)}(m)$ is available, as shown in the following listed formulas:

$$\begin{aligned} Q(s_{ii}, s_{kl}, m) &= (1 - v_{ii})^m \rho_{(i,i) \rightarrow (k,l)}(m), \\ Q(s_{ii}, s_F, m) &= (1 - v_{ii})^{m-1} v_{ii}, \\ Q(s_{ii}, s_{ii}, m) &= 0, \\ Q(s_{ij}, s_{kl}, m) &= \begin{cases} \rho_{(i,j) \rightarrow (k,l)}(m), & m \leq T_{hdij}, \quad k = l = i, \\ 0, & \text{otherwise,} \end{cases} \\ Q(s_{ij}, s_F, m) &= \begin{cases} 0, & m \leq T_{hdij}, \\ 1 - \sum_{m=1}^{T_{hdij}} Q(s_{ij}, s_{ii}, m), & m > T_{hdij}, \end{cases} \\ Q(s_F, s_F, m) &= \begin{cases} 1, & m = 1, \\ 0, & m > 1. \end{cases} \end{aligned} \quad (21)$$

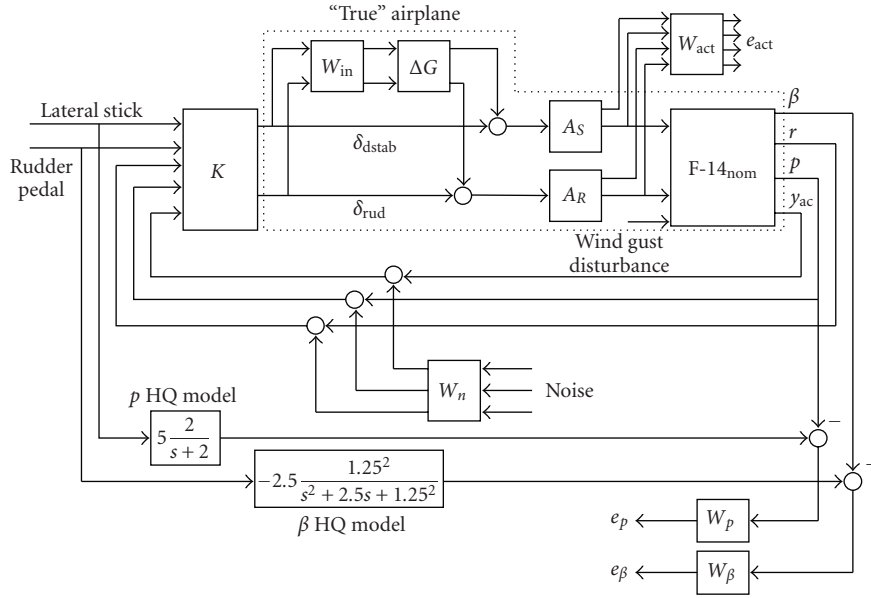


FIGURE 4: Control design diagram for F-14 lateral axis (Courtesy of The MathWorks, Inc.).

Although these formulas appear to be simpler, both the parameter estimation and competition probability calculations need much more calculation burden than the first case when FDI decision is modeled as a hypothetical Markov chain. Once X_n is constructed, calculation of reliability function and MTTF are straightforward using available formulas [9].

6. DEMONSTRATION ON AN F-14 AIRCRAFT MODEL

6.1. Model description

A control problem of F-14 aircraft was presented in [10], and also used as a demonstration example in MATLAB Robust Control Toolbox.¹ This problem considers the design of a lateral-directional axis controller during powered approach to a carrier landing with two command inputs from the pilot: lateral stick and rudder pedal. At an angle-of-attack of 10.5 degrees and airspeed of 140 knots, the nominal linearized F-14 model has four states: lateral velocity, yaw rate, roll rate, and roll angle, denoted by v , r , p , and ϕ , respectively, two control inputs: differential stabilizer deflection and rudder deflection, denoted by δ_{dstab} and δ_{rud} , respectively, and four outputs: roll rate, yaw rate, lateral acceleration, and side-slip angle, denoted by p , r , y_{ac} , and β , respectively. The system dynamics equations are ignored here, and can be loaded in MATLAB 7.1 using command “load F14nominal.” An additional disturbance input is added to represent the wind gust effects.

The control objective is to have desired handling quality (HQ) responses from lateral stick to roll rate p and from rudder pedal to side-slip angle β . Under fault-free modes, the

HQ models are $5(2/(s+2))$ and $-2.5(1.25^2/(s+2.5s+1.25^2))$; when fault occurs, HQ models degrade to $5(1/(s+1))$ and $-2.5(0.75^2/(s+1.5s+0.75^2))$, respectively.

The system block diagram is shown in Figure 4, where F_{14nom} represents the nominal linearized F-14 model, and A_S and A_R the actuator models. e_p and e_β represent the weighted model matching errors. Actuator energy is described by e_{act} , and noise is added to the measured output after antialiasing filters.

The considered fault occurs in two actuators. Under fault-free mode, their transfer functions are

$$A_S = A_R = \frac{25}{s+25}. \quad (22)$$

Two types of actuator faults are considered here, each has mean occurrence time 10^5 of FDI periods or its failure rate is 10^{-5} . Under fault type 1, the transfer function of A_S becomes

$$A'_S = 0.5 \frac{15}{s+15}. \quad (23)$$

Under fault type 2, the transfer function of A_R becomes

$$A'_R = 0.5 \frac{10}{s+10}. \quad (24)$$

These fault modes are described as the change of actuator gains and time constants. The set of fault modes is denoted by $S = \{0, 1, 2, 3\}$, representing fault-free, fault type 1, type 2, and simultaneous occurrence of both.

6.2. Performance characterization of controller and FDI

Four H_∞ controllers are designed for each fault mode to achieve nominal HQ control objectives under fault-free

¹ MATLAB and Robust Control Toolbox are the trademarks of The MathWorks, Inc.

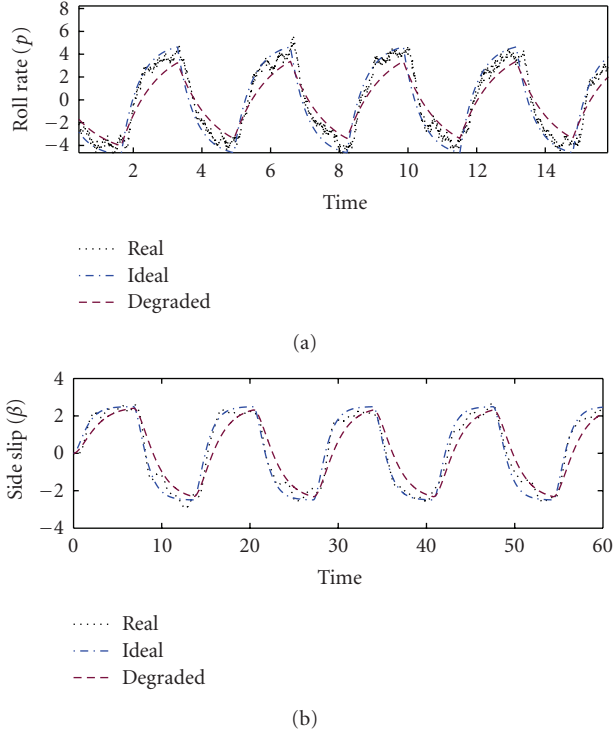


FIGURE 5: Output trajectories.

mode and degraded HQ performance under fault modes. Typical output trajectories under fault-free mode are shown in Figure 5, where the curves labeled with “Real” represent the measured outputs, “Ideal” the outputs under nominal HQ performance, and “Degraded” the outputs under degraded HQ performance. The absolute minimal matching errors between the real responses and the expected outputs under ideal HQ performance are shown in Figure 6, which are assumed to represent system safety behaviors. When these matching errors go over the safety limits, 30% of expected output, aircraft is considered as failed.

An IMM FDI is constructed to detect fault occurrences. To reduce false alarms, a steady-state test strategy is applied on FDI decisions with $T_{SSTj} = 6$ for any FDI mode j . A typical FDI trajectory is shown in Figure 7. It is clear that the steady FDI mode is free of false alarms in the shown time period. But detection time delays are introduced when fault occurs at 20 and 50 seconds, respectively.

To represent FDI detection characteristics, a batch of fault and FDI history data is collected for statistical estimation. First, histograms of FDI delays are generated to check its distribution type. When there is no fault, the histogram of FDI sojourn time at fault-free mode is shown in Figure 8. It clearly resembles a geometric distribution. Equations (10)-(11) are then used to estimate Markov transition probabilities, and those under fault-free mode are obtained as

$$H^0 = \begin{bmatrix} 0.9990 & 0 & 0.0010 & 0.0000 \\ 1.0000 & 0 & 0 & 0 \\ 0.1330 & 0 & 0.8670 & 0 \\ 0.5000 & 0 & 0 & 0.5000 \end{bmatrix}. \quad (25)$$

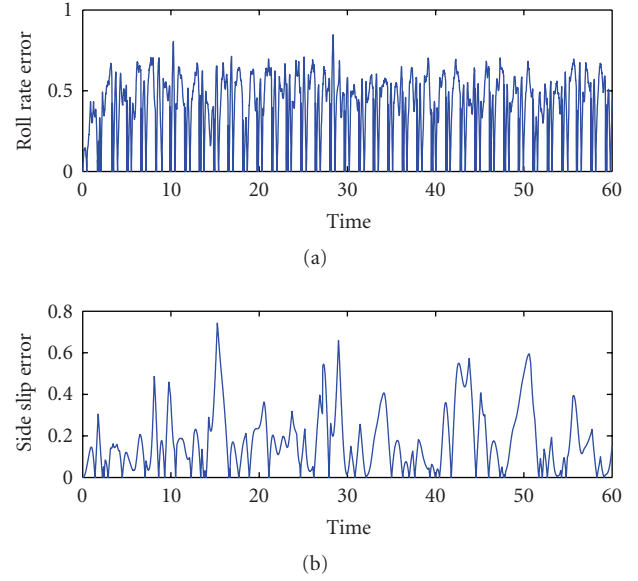


FIGURE 6: The trajectories of matching errors.

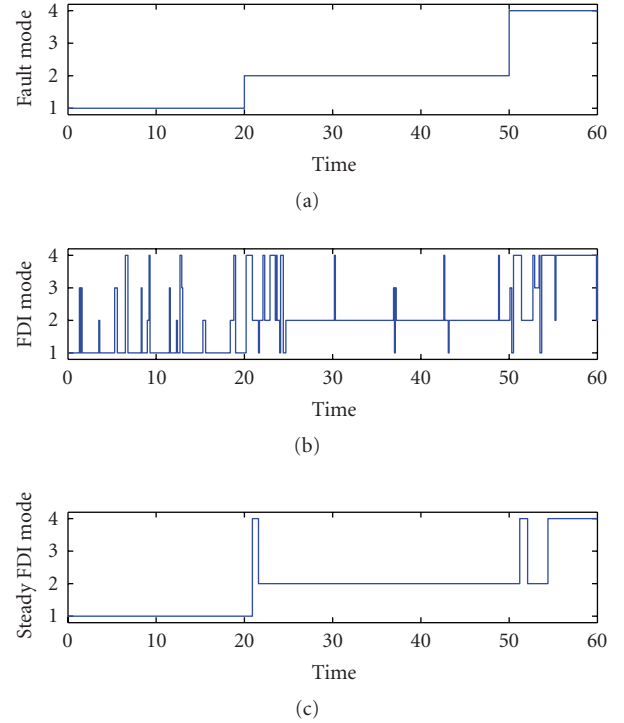


FIGURE 7: FDI trajectory.

Note that $H^0(2, 1) = 1$ and $H^0(2, 2) = 0$ represent the transition probabilities of FDI from a false alarm state. Estimated based on the given history data, these values imply that the FDI leaves false alarm state in one transition cycle. But there may exist estimation error, and the true value of $H^0(2, 2)$ may be close to but not exact zero.

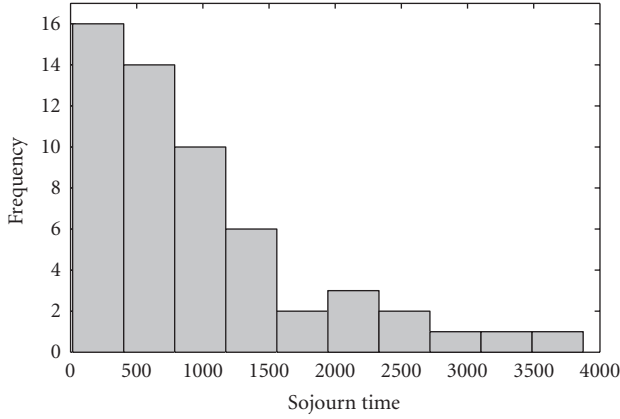


FIGURE 8: Histogram of FDI sojourn time.

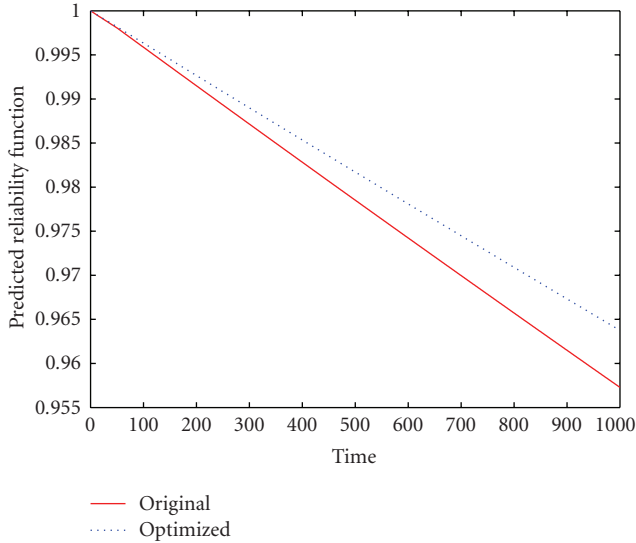


FIGURE 9: Reliability functions comparison.

As a result of FDI false alarms, missing detections, and detection delays, controllers may be engaged for various fault modes for which they are not designed. So, it is necessary to evaluate system behavior under all possible combinations of FDI and fault modes. Here, Monte Carlo simulations are adopted with the following settings: (1) command stick inputs are square waves with frequency as a random variable ranging from 0.2 to 2 Hertz, (2) wind gust disturbances and sensor measurement noises are assumed to be Gaussian processes, (3) actuator saturation effects limit control inputs to 20 and 30, respectively, (4) system failure is assumed to occur when model matching errors go over 30% of stick commands. For example, with fault mode 2 occurred and \mathcal{K}_2 engaged, mean time to system failure is 57 403 seconds when controller \mathcal{K}_2 is used, and 6 seconds when \mathcal{K}_1 is used. Considering the sampling period to be 0.1 second for IMM FDI, the outcrossing failure rate and hard-deadline are $\nu_{22} = 1/574030$, $T_{hd21} = 60$.

6.3. Reliability evaluation

Reliability semi-Markov model can be constructed based on fault transition rates, FDI transition parameters, outcrossing failure rate, and hard-deadlines. Predicted reliability function and MTTF can be thereby calculated. By using MTTF as an objective, an optimization is performed on T_{SST} . It is found that MTTF will be improved from 27 727 to 32 605 seconds if T_{SSTj} is reduced from 6 to 1. A comparison of reliability functions before and after this optimization is shown in Figure 9. It is clearly shown that reliability index is improved.

Comparisons on the transition probabilities between these two SST periods are shown in Figure 10, in which each subfigure gives the transition probability curves from s_{00} to other states. For example, the subfigure at the first row and second column shows that the transition probabilities to s_{01} are increased from 0 to about 0.008. This is a natural result of increased false alarms when reducing T_{SSTj} . In fact, when $T_{SSTj} = 1$, new Markov transition parameters H'^0 become

$$H'^0 = \begin{bmatrix} 0.9822 & 0.0017 & 0.0122 & 0.0038 \\ 0.2634 & 0.7366 & 0 & 0 \\ 0.1989 & 0 & 0.8011 & 0 \\ 0.3530 & 0 & 0 & 0.6470 \end{bmatrix}. \quad (26)$$

Compared with H^0 , the element on the first row and second column is increased from 0 to 0.0017, a confirmation of increased false alarms. On the other hand, detection delays are reduced approximately from 6 to 1, and system stays less time under mismatched fault and FDI cases. Overall, MTTF is improved.

This evaluation procedure can be completed in an online manner. Estimated FDI transition parameters H and current mode of ζ_n provided by confirmed test on FDI can be used to provide updated MTTF based on this most recent information.

7. CONCLUSIONS

A reliability monitoring scheme for FTCs is reported in this paper. The scheme contains two postprocessing strategies on FDI results to provide estimated fault mode for control re-configuration and confirmed mode for updating reliability. The stochastic transitions of FDI mode is represented by a semi-Markov chain with parameters estimated from history data. Under geometric sojourn time distributions, FDI mode can be described by an equivalent hypothetical Markov chain that simplifies its model and reliability analysis. Safety and satisfactory operation of system is defined by system trajectories and safety boundaries; the probability of violating this safety criterion under fixed fault and FDI modes is estimated using Monte Carlo simulations. Overall reliability evaluation is obtained through a semi-Markov model constructed by integrating FDI transition characteristics and failure probabilities under each regime model. This scheme provides timely monitoring on the reliability index of FTCs, and was demonstrated on an F-14 aircraft model.

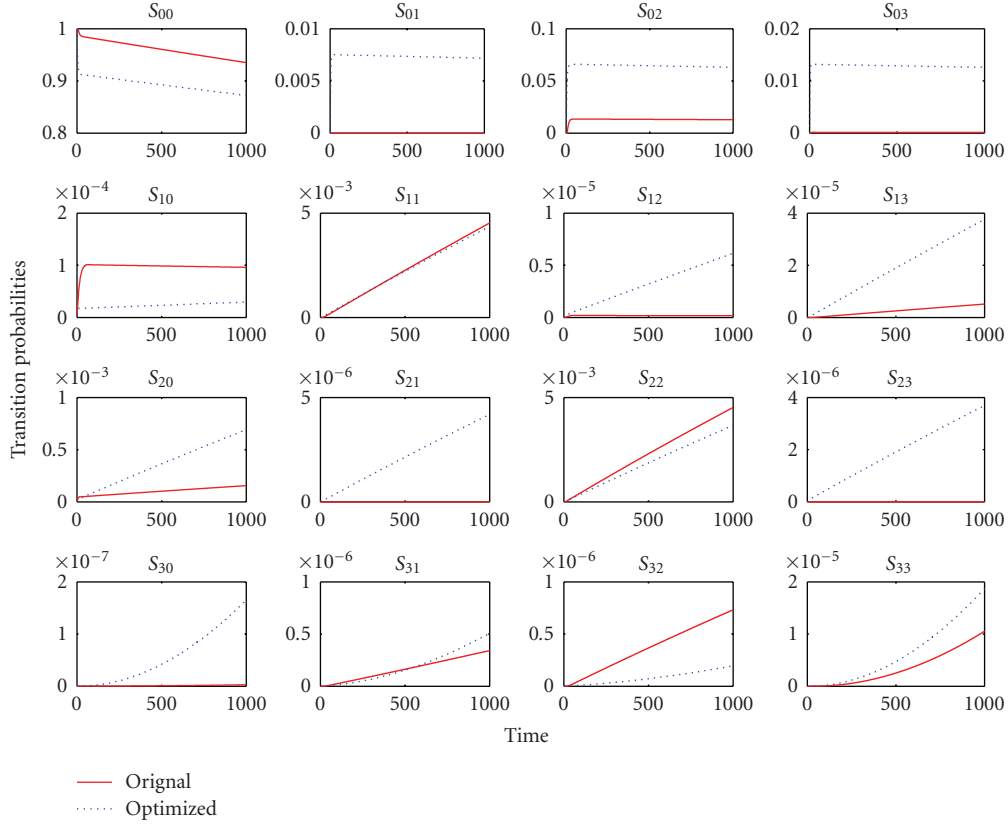


FIGURE 10: Comparison of transition probabilities.

APPENDIX

Proof of Lemma 1. The “only if” part is trivial as shown in (8). Let η_n denote a semi-Markov chain; the associated Markov renewal processes are denoted as θ_m and T_m , and the sojourn time distribution h_i^k when subsequent state is not specified is in geometric distribution:

$$\begin{aligned} \Pr\{\eta_{n+1} = j \mid \eta_1, \dots, \eta_n\} \\ = \Pr\{\eta_{n+1} = j \mid \theta_1, \dots, \theta_{S_n}, T_1, \dots, T_{S_n}\}. \end{aligned} \quad (\text{A.1})$$

If $\theta_{S_n} = j$,

$$\begin{aligned} \Pr\{\eta_{n+1} = j \mid \eta_1, \dots, \eta_n\} \\ = \Pr\{T_{S_{n+1}} > n+1 \mid \theta_1, \dots, \theta_{S_n}, T_1, \dots, T_{S_n}, T_{S_{n+1}} > n\} \\ = \Pr\{T_{S_{n+1}} > n+1 \mid \theta_{S_n}, T_{S_n}, T_{S_{n+1}} > n\} \\ = \Pr\{T_{S_{n+1}} - T_{S_n} > n+1 - T_{S_n} \mid \theta_{S_n}, T_{S_n}, T_{S_{n+1}} > n - T_{S_n}\} \\ = \Pr\{T_{S_{n+1}} - T_{S_n} > 1 \mid \theta_{S_n}\} \\ = \Pr\{\eta_{n+1} = j \mid \eta_n\}; \end{aligned} \quad (\text{A.2})$$

otherwise, $\theta_{S_n} \neq j$, and we have

$$\begin{aligned} \Pr\{\eta_{n+1} = j \mid \eta_1, \dots, \eta_n\} \\ = \Pr\{\theta_{S_{n+1}} = j, T_{S_{n+1}} = n+1 \mid \theta_1, \dots, \theta_{S_n}, \\ T_1, \dots, T_{S_n}, T_{S_{n+1}} > n\} \\ = \Pr\{\theta_{S_{n+1}} = j, T_{S_{n+1}} = n+1 \mid \theta_{S_n}, T_{S_n}, T_{S_{n+1}} > n\} \\ = \Pr\{\theta_{S_{n+1}} = j, T_{S_{n+1}} - T_{S_n} = n+1 - T_{S_n} \mid \theta_{S_n}, \\ T_{S_{n+1}} - T_{S_n} > n - T_{S_n}\} \\ = \Pr\{\theta_{S_{n+1}} = j, T_{S_{n+1}} - T_{S_n} = 1 \mid \theta_{S_n}\} \\ = \Pr\{\eta_{n+1} = j \mid \eta_n\}. \end{aligned} \quad (\text{A.3})$$

In the above derivations, the memoryless property of geometric distributions has been used:

$$\begin{aligned} \Pr\{T_{S_{n+1}} - T_{S_n} > n+1 - T_{S_n} \mid T_{S_{n+1}} - T_{S_n} > n - T_{S_n}\} \\ = \Pr\{T_{S_{n+1}} - T_{S_n} > 1\}, \\ \Pr\{T_{S_{n+1}} - T_{S_n} = n+1 - T_{S_n} \mid T_{S_{n+1}} - T_{S_n} > n - T_{S_n}\} \\ = \Pr\{T_{S_{n+1}} - T_{S_n} = 1\}. \end{aligned} \quad (\text{A.4})$$

The Markov property of η_n is proved, so η_n is a Markov chain. \square

REFERENCES

- [1] N. E. Wu, "Coverage in fault-tolerant control," *Automatica*, vol. 40, no. 4, pp. 537–548, 2004.
- [2] B. Walker, "Fault tolerant control system reliability and performance prediction using semi-Markov models," in *Proceedings of Safeprocess*, pp. 1053–1064, Kingston Upon Hull, UK, 1997.
- [3] H. Li, Q. Zhao, and Z. Yang, "Reliability modeling of fault tolerant control systems," to appear in *International Journal of Applied Mathematics and Computer Science*.
- [4] H. Li and Q. Zhao, "Reliability evaluation of fault tolerant control with a semi-Markov fault detection and isolation model," *Proceedings of the Institution of Mechanical Engineers Part I*, vol. 220, no. 5, pp. 329–338, 2006.
- [5] J. Song and A. Der Kiureghian, "Joint first-passage probability and reliability of systems under stochastic excitation," *Journal of Engineering Mechanics*, vol. 132, no. 1, pp. 65–77, 2006.
- [6] Y. Zhang and X. R. Li, "Detection and diagnosis of sensor and actuator failures using IMM estimator," *IEEE Transactions on Aerospace and Electronic Systems*, vol. 34, no. 4, pp. 1293–1313, 1998.
- [7] W. Kuo and M. Zuo, *Optimal Reliability Modeling*, John Wiley & Sons, Hoboken, NJ, USA, 2002.
- [8] R. V. Field Jr. and L. A. Bergman, "Reliability-based approach to linear covariance control design," *Journal of Engineering Mechanics*, vol. 124, no. 2, pp. 193–199, 1998.
- [9] V. Barbu, M. Boussemart, and N. Limnios, "Discrete-time semi-Markov model for reliability and survival analysis," *Communications in Statistics: Theory and Methods*, vol. 33, no. 11, pp. 2833–2868, 2004.
- [10] G. J. Balas, A. K. Packard, J. Renfrow, C. Mullaney, and R. T. M'Closkey, "Control of the F-14 aircraft lateral-directional axis during powered approach," *Journal of Guidance, Control, and Dynamics*, vol. 21, no. 6, pp. 899–908, 1998.

